

SOME PHENOMENOLOGICAL ASPECTS OF KAON PHOTOPRODUCTION IN THE EXTREME KINEMATICS*

S. SAKINAH, S. CLYMTON, T. MART

Departemen Fisika, FMIPA, Universitas Indonesia, Depok 16424, Indonesia

(Received November 16, 2018; accepted May 9, 2019)

We have investigated phenomenological aspects of kaon photoproduction in three different extreme kinematics. The first kinematics of interest is the threshold region. At the threshold, we have investigated the convergence of kaon photoproduction amplitude by expanding the square of the amplitude in terms of the ratio m_K/m , where m_K is the mass of kaon and m is the averaged mass of nucleon and Λ hyperon. The amplitude is calculated from the appropriate Feynman diagrams by using the pseudovector theory. The contact diagram as a consequence of the PCAC hypothesis is also taken into account in the amplitude. Our finding indicates that the convergence can only be achieved if the amplitude was expanded up to the at least 12th order. As a consequence, applications of some theoretical calculations based on the expansion of the scattering amplitude, such as the Low Energy Theorem or Soft Kaon Approximation, cannot be easily managed in kaon photoproduction. The second kinematics is the forward region, where we could assume only t -channel contributes to the process. Here, we have investigated the effect of amplitude expansion on the extraction of the coupling constants $g_{K^+\Lambda p}$ and $g_{K_1^+\Lambda p}^V$. The last kinematics is the backward region, where we have also assumed that only u -channel survives and we could extract the leading coupling constants $g_{K^+\Lambda p}$ and $g_{K^+\Sigma^0 p}$.

DOI:10.5506/APhysPolB.50.1389

1. Introduction

In the previous works, we have studied kaon photo- and electroproduction near their production thresholds by using the pseudoscalar (PS) and pseudovector (PV) theories [1, 2]. Extended studies to cover not only the threshold energy but also the resonance region have been also performed [3–5]. These studies indicate that compared to the PV coupling, the PS one leads to a better agreement with experimental data. This is the reason that the PS coupling is commonly used in the phenomenological investigations of

* Funded by SCOAP³ under Creative Commons License, CC-BY 4.0.

kaon photoproduction. We note, however, that this is not the case in pion production, where the PV coupling can be and is mostly used in the production formalism. The reason is that the cross section of kaon production obtained in experiments is two order of magnitude smaller than that of pion production, whereas the Feynman diagrams and the coupling constants used in the theoretical formulation of both processes are similar. Since in photoproductions the pion thresholds are the lowest, pion photoproduction has been used as the main reaction for investigating the Low Energy Theorem (LET) [6, 7]. LET is derived by using the PV coupling and expanding the pion photoproduction amplitude in terms of the ratio of pion and nucleon masses. Since this ratio is considerably small and the expansion can quickly converge, terms with higher orders can be obviously neglected. We also note that the successful Chiral Perturbation Theory formulation assumes that pion is a pseudovector particle.

On the other hand, kaon mass is much heavier than pion mass. Therefore, for kaon photoproduction, LET has not been seriously considered since the convergence cannot be easily achieved. However, an attempt to derive LET for the radiative decay width of charged kaon $K \rightarrow l + \nu + \gamma$ within the so-called Soft Kaon Approximation (SKA) was performed more than five decades ago [8]. Comparison with the result obtained from the Pole Dominance Approximation [9] reveals the fact that the result of the SKA is shifted upward by approximately 20%. Such a significant difference indicates that further studies of SKA are strongly required. Presumably, the problem originates from the intrinsic properties of kaon as compared to the pion, *e.g.*, the heavier mass of kaon. A systematic and careful investigation of the convergence of kaon scattering amplitude is therefore very important to this end. As a first step, we might investigate the convergence of kaon photoproduction amplitude, for which experimental data are abundant nowadays.

Furthermore, kaon photoproduction at forward and backward angles is also of interest, since at the two extreme directions contributions of t - and u -channels it would be dominant. As a consequence, theoretical formulation of kaon photoproduction in both cases could be extremely simplified. This is valid not only in kaon photoproduction, but also in the electromagnetic production of meson in general. For instance, in Ref. [10], it is shown that it is possible to extract the pion electromagnetic form factor by merely using the t -channel diagram, provided that only the pion electroproduction data obtained in the forward direction are used in the analysis. It is also important to mention here that forward angles are very decisive for hypernuclear production, since only in this kinematics the nuclear cross section is sufficiently large. The nuclear form factor suppresses this cross section strongly as the kaon scattering angle increases. Since the elementary operator for

this purpose is constructed from the kaon photoproduction amplitude, an accurate description for the forward angles production is inevitable [11]. To check whether or not the u -channel contribution dominates the kaon photoproduction amplitude, measurement of kaon photoproduction at backward angles was also performed at SPring8 more than a decade ago [12].

In this paper, we investigate the convergence of kaon photoproduction amplitude by expanding the squared amplitude, which is proportional to the cross section, in terms of the ratio m_K/m , where m_K is the mass of kaon and m is the averaged mass of nucleon and Λ hyperon. For this purpose, we construct the minimal model that can explain experimental data very close to the threshold. We use the suitable Feynman diagrams with PV coupling based on our previous studies [1, 2]. The analytic calculation of the amplitude expansion was performed with the help of **Mathematica** software. The same method is also used to derive the reaction amplitudes in the forward and backward angles.

This paper is organized as follows. In Sec. 2, we present the kinematics of the photoproduction process. Section 3 discusses the expansion of the photoproduction amplitude in general. The corresponding numerical result is given in Sec. 4. Section 5 is devoted to the discussion of kaon photoproduction in the forward region. The case of backward angles photoproduction is given in Sec. 6. We will summarize our finding in Sec. 7. The expansion of the photoproduction amplitude up to the 9th order is given in Appendix A.

2. Kinematics

Let us consider the kaon photoproduction process

$$\gamma(k) + p(p_p) \longrightarrow K^+(q) + \Lambda(p_\Lambda), \tag{1}$$

where the four-momenta of the photon γ , proton p , kaon K^+ and Λ hyperon are explicitly indicated.

To derive the photoproduction amplitude, we use the first order Feynman diagrams shown in Fig. 1. Following the previous works on pion photoproduction, here we consider kaon as a pseudovector particle, instead of pseudoscalar one. As will be explained in the next section, the choice is also supported by the fact that the expansion of the PS amplitude has a serious problem since the PS amplitude contains the large $\mathcal{O}(m/m_K)$ terms, instead of the small and expandable $\mathcal{O}(m_K/m)$ terms. The conservation of axial-vector current requires the kaon to be massless. Therefore, at $m_K \rightarrow 0$ and $q = 0$ (at threshold), the amplitude to the first order of electromagnetic coupling can be written as

$$\mathcal{M}(m_K \rightarrow 0, q = 0) = \bar{u}_\Lambda(p_\Lambda) \left[-\frac{g_{K^+\Lambda p}}{m_p + m_\Lambda} \gamma_5 \not{\epsilon} \right] u_p(p_p). \tag{2}$$

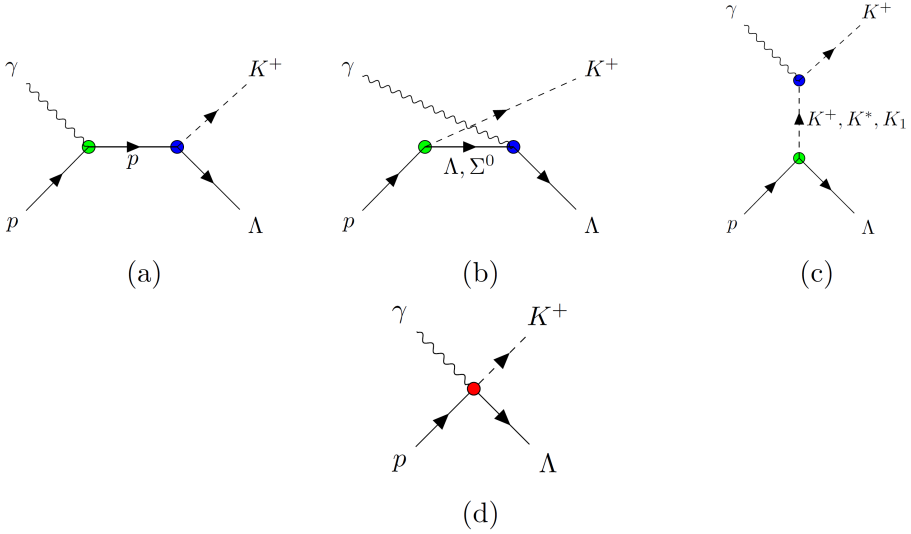


Fig. 1. Feynman diagrams for the Born terms of the $K^+\Lambda$ photoproduction. The corresponding s -, u -, and t -channels are shown by diagrams (a), (b), and (c), respectively, whereas the contact (seagull) term is given by diagram (d).

This term is known as the contact (seagull) term, which contributes in the zeroth order of amplitude and is considered as a consequence of the partially conserved axial current (PCAC) hypothesis [13]. Besides the Born and contact terms, we also include two more intermediate states that have been proven to be important to achieve a better agreement with experimental data. They are the K^* and K_1 vector-meson resonances. The total amplitude reads

$$\begin{aligned}
 \mathcal{M} = & \bar{u}_\Lambda(p_\Lambda) \left[i \frac{g_{K^+\Lambda p}}{m_\Lambda + m_p} \gamma_5 \not{q} \frac{\not{p} + \not{k} + m_p}{s - m_p^2} (e\not{\epsilon} + i\sigma^{\mu\nu} \epsilon_\mu k_\nu \mu_p) \right. \\
 & + i\sigma^{\mu\nu} \epsilon_\mu k_\nu \mu_\Lambda \frac{\not{p}_\Lambda - \not{k} + m_\Lambda}{u - m_\Lambda^2} \frac{ig_{K^+\Lambda p}}{m_\Lambda + m_p} \gamma_5 \not{q} \\
 & + ie \frac{g_{K^+\Lambda p}}{m_\Lambda + m_p} \gamma_5 (\not{q} - \not{k}) \frac{2q\epsilon}{t - m_k^2} - \frac{g_{K^+\Lambda p}}{m_p + m_\Lambda} \gamma_5 \not{\epsilon} \\
 & \left. + \frac{i}{M(t - m_{K^*}^2 + im_{K^*}\Gamma_{K^*})} \left\{ g_{K^*\Lambda p}^V \gamma_\mu - \frac{g_{K^*\Lambda p}^T}{m_p + m_\Lambda} i\sigma^{\mu\nu} (q_K - k)_\nu \right\} \right. \\
 & \left. \times i\epsilon_{\mu\nu\rho\sigma} \epsilon^\nu k^\rho q_K^\sigma g_{K^*K+\gamma} + \frac{i}{M(t - m_{K_1}^2 + im_{K_1}\Gamma_{K_1})} \left\{ g_{K_1\Lambda p}^V \gamma^\mu \gamma_5 \right\} \right]
 \end{aligned}$$

$$\begin{aligned}
 & + \frac{g_{K_1\Lambda p}^T}{m_p + m_\Lambda} \left(\not{p}_\Lambda - \not{p}_p \right) \gamma^\mu \gamma_5 \left\{ (q_K \epsilon k_\mu - q_K k \epsilon_\mu) g_{K_1 K+\gamma} \right. \\
 & \left. + i\sigma^{\mu\nu} \epsilon_\mu k_\nu \mu_T \frac{\not{p}_\Sigma - \not{k} + m_\Sigma}{u - m_\Sigma^2} \frac{i g_{K+\Sigma^0 p}}{m_\Sigma + m_p} \gamma_5 \not{q} \right] u_p(p_p), \tag{3}
 \end{aligned}$$

where ϵ is the photon polarization, μ_p and μ_Λ represent the magnetic moments of proton and Λ hyperon, respectively, while s , t and u indicate the Mandelstam variables. In Eq. (3), we have introduced $M = 1$ GeV to make the transition strengths $g_{K^*K+\gamma}$ and $g_{K_1K+\gamma}$ dimensionless. Note that since in the phenomenological studies of kaon photoproduction the two transition strengths cannot be explicitly separated, we define $G_{K^*}^{V,T} = g_{K^*K+\gamma} g_{K^*\Lambda p}^{V,T}$ and $G_{K_1}^{V,T} = g_{K_1K+\gamma} g_{K_1\Lambda p}^{V,T}$.

For the calculation of cross section with the full amplitude, it is customary to decompose the transition amplitude in Eq. (3) into the gauge and Lorentz invariant matrices M_j , *i.e.*, [14]

$$\mathcal{M} = \bar{u}(p_\Lambda) \sum_{j=1}^4 A_j(s, t, u) M_j u(p_p), \tag{4}$$

where

$$M_1 = \gamma_5 \not{k}, \tag{5}$$

$$M_2 = 2\gamma_5 (q \epsilon P k - q k P \epsilon), \tag{6}$$

$$M_3 = \gamma_5 (q k \not{\epsilon} - q \epsilon \not{k}), \tag{7}$$

$$M_4 = i\epsilon_{\mu\nu\rho\sigma} \gamma^\mu q^\nu \epsilon^\rho k^\sigma, \tag{8}$$

with $P = (p_p + p_\Lambda)/2$ and $\epsilon_{\mu\nu\rho\sigma}$ the Levi-Civita tensor. The form functions A_i given in Eq. (4) can be used to calculate the cross section.

The transition amplitude \mathcal{M} in Eq. (3) can be also written within the PS theory by replacing $g_{K+\Lambda p} \gamma_5 \not{q} / (m_\Lambda + m_p)$ in the s - and u -channels and $g_{K+\Lambda p} \gamma_5 (\not{q} - \not{k}) / (m_\Lambda + m_p)$ in the t -channel with $g_{K+\Lambda p} \gamma_5$ [1]. However, it is found that the expansion of the PS amplitude is difficult because the expansion contains the terms that are proportional to x^{-1} , where $x = m_K/m$. Thus, to achieve the convergence is a daunting task in this case. The problem originates from the fact that in the PS theory the amplitude is not proportional to the kaon momentum q , as in the case of PV theory [see Eq. (3)].

3. Expansion of the amplitude

The transition amplitude of kaon photoproduction obtained from the Feynman diagrams shown in Fig. 1 is given in Eq. (3). The form functions A_i are intended for the calculation of the cross section in the data fitting as well as for obtaining the result of full calculation which will be compared with the approximations made in the present work [1]. Since we limit our study to energies very close to the threshold, we do not use nucleon resonances in our calculation. The latter is also important to significantly simplify the amplitude formulation.

There are very few experimental data points near the threshold, as will be shown in the next section. The closest ones to the threshold are obtained from the SAPHIR data [15]. Since we exclude the nucleon resonances, the calculated full amplitude in the present calculation differs from our previous model [1]. As a consequence, we must refit the coupling constants in order to obtain a reasonable amplitude. The result is shown in Table I, where we compare our present result with that of the previous PV calculation [1]. From Table I, it appears that the coupling constants obtained from refitting the experimental data differ, although not dramatically, from those of previous work. The larger value of χ^2/N obtained in the present work is understandable because the number of free parameters decreases due to the exclusion of nucleon and hyperon resonances.

TABLE I

Coupling constants extracted from fittings to experimental data in the previous [1] and present works and the corresponding χ^2/N .

Coupling constant	Previous	Present
$g_{K^+ \Lambda p} / \sqrt{4\pi}$	-3.80	-3.00
$g_{K^+ \Sigma^0 p} / \sqrt{4\pi}$	1.20	1.30
$G_{K^*}^V / 4\pi$	-0.79	-0.73
$G_{K^*}^T / 4\pi$	-0.04	0.70
$G_{K_1}^V / 4\pi$	1.19	0.80
$G_{K_1}^T / 4\pi$	-0.68	-1.50
χ^2/N	1.526	1.739

The square of photoproduction amplitude is expanded in terms of the ratio between kaon and baryon masses in the reaction. Different from the pion photoproduction, in the kaon photoproduction, the baryon in the initial and final states are proton and Λ hyperon, respectively. Therefore, we define the baryon mass m as the average of the proton mass m_p and Λ -hyperon mass

m_A , and the ratio becomes $x = m_K/m = 2m_K/(m_p + m_A)$. Furthermore, to simplify the formalism, in the present work, we also make the assumption that $m_p \approx m_A$.

In this work, the expansion of the square of amplitude has been performed up to $n = 20$, in order to reach the convergence. The expansion has been done analytically with the help from the **Mathematica** software. We calculate the expansion of the squared amplitude instead of the amplitude itself because we find it is more simple and practical to use and to compare with experimental data as well as the result of other calculations. We are aware that there exist a number of studies which compare the results with multipoles amplitudes. Nevertheless, for this exploratory study, we limit our calculation to the total cross section. At the threshold, the (reduced) total cross section of kaon photoproduction can be written as

$$\frac{|\mathbf{k}|}{|\mathbf{q}|} \sigma_{\text{tot}} = \frac{1}{64\pi s} |\mathcal{M}|^2 \quad (9)$$

with

$$|\mathcal{M}|^2 = \sum_{n=0}^{20} |\mathcal{M}|_{(n)}^2 = |\mathcal{M}|_{(0)}^2 + |\mathcal{M}|_{(1)}^2 + |\mathcal{M}|_{(2)}^2 + \dots, \quad (10)$$

where the subscript indicates the order of expansion. Therefore, $|\mathcal{M}|_{(n)}^2 \propto x^n$. The formulas of $|\mathcal{M}|_{(n)}^2$ with n up to 9 are given in Appendix A. For higher order amplitudes, the formulas are very complicated and too long to be written in this paper, although it is produced by **Mathematica** and relatively simple for numerical computation. Nevertheless, for the sake of completeness in the present work, we still calculate the cross section with n up to 20, in spite of the fact that to reach the convergence, the number of order is significantly less than 20, as will be discussed in the next section.

4. Numerical results

The momentum and energy distributions of the calculated reduced total cross section are shown in Fig. 2, where we also compare the result of previous calculations obtained by using PS and PV couplings [1] along with the available experimental data [16]. As discussed above as well as in Ref. [1], the PS model yields a better agreement with experimental data. This is clearly shown in Fig. 2. Furthermore, we can also see that the PV model without hyperon and nucleon resonances produces a slightly different cross section compared to the full calculation. This result indicates that without hyperon and nucleon resonances, the PV model can still nicely work and

provide a good framework for the purpose of comparison with the present work. Furthermore, from Fig. 2, we find that the calculated reduced total cross section at threshold is around $0.65 \mu\text{b}$. This is clearly smaller than the experimental data near the threshold. However, we also observe that the experimental error bar in this case is significantly large. Thus, we still believe that for the sake of comparison made in the present work, Fig. 2 justifies that we can use the simplified model, *i.e.*, the model constructed from Born terms along with the K^* and K_1 vector mesons.

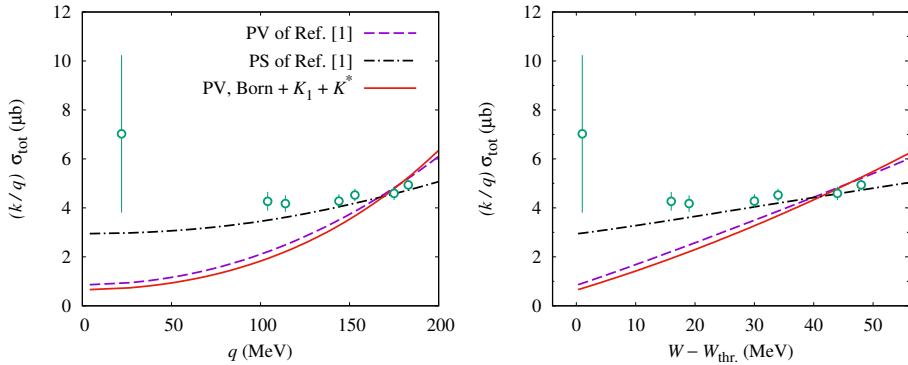


Fig. 2. Reduced total cross section as a function of the kaon three-momentum $q = |\mathbf{q}|$ (left panel) and the total c.m. energy above the threshold energy (right panel) obtained by using the PV (dashed lines) and PS (dot-dashed lines) couplings, where the Born, K^* , K_1 , hyperon, and nucleon resonance terms are included [1]. Solid lines are obtained from the calculation that includes the Born, K^* , and K_1 terms only. Open circles indicate the CLAS 2006 data [16].

By using the PV model with parameters given in the third column of Table I and the particle properties taken from the Particle Data Group (PDG) listed in Table II, we calculate the reduced total cross section at threshold for each of the expansion order. The result is listed in Table III and graphically displayed as a function of n (order of expansion) in Fig. 3, where the solid thick/green line indicates the full order calculation as our reference value. From Table III and Fig. 3, it is apparent that the lowest order calculation yields very large discrepancy with the full calculation. Figure 3 shows that the expansion starts to converge at the 9th order. Although at this order a small discrepancy still exists (about 6%), we have also to admit that we have made an assumption for baryonic mass m , which could also create sizable error.

TABLE II

Properties of the particles considered in this study [17].

Particle	S	J^P	I	μ [n.m.]	Mass [MeV]	Width [MeV]
p	0	$\frac{1}{2}^+$	$\frac{1}{2}$	2.79284734	938.2721	—
n	0	$\frac{1}{2}^+$	$\frac{1}{2}$	-1.91304273	939.5654	—
K^+	1	0^-	$\frac{1}{2}$	—	493.677	—
Σ^0	-1	$\frac{1}{2}^+$	1	1.61 ± 0.08	1192.642	—
Λ	-1	$\frac{1}{2}^+$	0	-0.613 ± 0.004	1115.683	—
K^{*+}	1	1^-	$\frac{1}{2}$	—	891.76 ± 0.25	50.3 ± 0.8
K_1	1	1^+	$\frac{1}{2}$	—	1272 ± 7	90 ± 20

TABLE III

Contribution of the n^{th} order photoproduction amplitude to the cross section at threshold.

Order of the expansion	Cross section [μb]
0 th	33.98
1 st	19.38
2 nd	-37.89
3 rd	-10.58
4 th	12.56
5 th	-2.96
6 th	-0.31
7 th	1.78
8 th	0.03
9 th	0.53
10 th	0.66
11 th	0.47
12 th	0.54
13 th	0.55
14 th	0.53
15 th	0.53
...	...
20 th	0.53

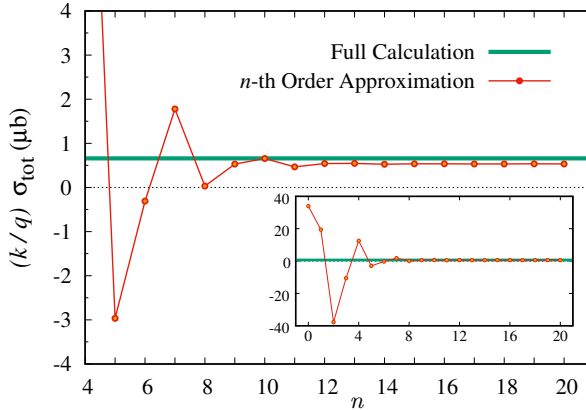


Fig. 3. (Color online) Convergence of the reduced total cross section as a function of the number of order of the expansion (n) with $n > 4$. The solid thin/red line indicates the approximated total cross section, whereas the solid thick/green line shows the result of full calculation. The inset displays the similar comparison but started with $n \geq 0$.

The result discussed above indicates that compared to the case of pion photoproduction, the LET for kaon photoproduction would require higher order terms. Actually, by excluding the K^* and K_1 contributions, we can achieve the convergence relatively faster, *i.e.*, it converges at the $n = 7$ order. However, it is well-known that the Born terms alone cannot reproduce the kaon photoproduction data, even near the threshold. This is in contrast to the pion photoproduction case. Note that in this work, we expand the square of amplitude instead of the amplitude itself. As a consequence, it is natural if the order of expansion required in the first case is twice larger than that of the second case. Nevertheless, as we explained above, the convergence of this squared amplitude is reached with $n = 9$. Therefore, the convergence of linear amplitude would be reached with $n > 4$. This is still not comparable to the case of pion photoproduction.

The expansion of squared amplitude given in Appendix A reveals the fact that there are zeroth order and first order squared amplitudes that depend solely on the coupling constant g_{K+Ap} [see Eqs. (A.11) and (A.12)]. Should we propose a LET by using only these term, as in the case of pion photoproduction, then we would find that the value of g_{K+Ap} must be much smaller than the prediction of SU(3) symmetry if the calculated cross section must be comparable to experimental data. The reason is that the cross section of kaon photoproduction is much smaller than that of the pion one. To sum up, we can safely say that the theories which are based on low order expansion of kaon mass, such as SKA and Chiral Perturbation Theory, should include higher order terms in order to produce the experimental data.

Should we try to create a LET by using higher order terms in our formalism, then the main problem would be the number of unknown parameters. We can also see that the expansion described above reduces the number of unknown parameters, *i.e.*, the coupling constants of K_1 and K^* intermediate states. From Eq. (3), we see that there are two coupling constants for each of them. From our assumption to generalize the baryonic masses, *i.e.*, $m_p \equiv m_\Lambda \equiv m$, the two couplings reduces to only one coupling [see Eqs. (A.9) and (A.10)]. As a result, in this formalism, we have only four unknown coupling constants. Nevertheless, it is by no means easy to derive LET from these 4 parameters. We have to find other mechanisms to reduce them. This is the interest of our future study, *i.e.*, to create higher order LET for kaon photoproduction. Furthermore, in the future, we will consider the expansion of amplitude, instead of the squared one described in the present work.

5. Kaon photoproduction in the forward direction

It is well-known that in the forward direction, the denominator of the t -channel propagator ($t - m_K^2$) is small. As a consequence, the corresponding propagator becomes large and the t -channel contribution dominates the production amplitude. The total amplitude given by Eq. (3) can be reduced and the unknown parameters can be limited to the coupling constants $g_{K+\Lambda p}$ and $g_{K_1^+\Lambda p}^V$ only. Since very close to the threshold there exist no experimental data in the forward angles, we extend the model to cover the resonance region, where $|\mathbf{q}| \neq 0$.

It is important to note that the t -channel exchange is not individually gauge-invariant. In the PV coupling theory, the nucleon exchange in the s -channel and the contact term must be included to restore the gauge invariance. In the PS coupling, the electric part of the s -channel alone is sufficient to restore the gauge invariance. This is in contrast to the anomalous magnetic moment part, which is already gauge-invariant by design, but not included in this work [18].

In the present analysis, we only have the coupling $g_{K+\Lambda p}$ as the unknown parameter, which can be directly extracted by fitting the model prediction to the experimental cross section obtained from the CLAS and LEPS collaborations. To this end, the closest available data are within $18^\circ < \theta < 25^\circ$. The result of extraction is listed in Table IV, where we can see that the coupling constant is relatively consistent to all orders. As expected, the χ^2/N decreases as we go to higher orders. Actually, the sign of the coupling $g_{K+\Lambda p}$ cannot be determined from the fitting process because the amplitude is calculated from the squared of the coupling. Therefore, we fix the sign by using the SU(3) prediction [19], although Table IV exhibits that the

extracted value is smaller than the SU(3) prediction by almost 50%. Nevertheless, we also note that such values were commonly obtained in the kaon photoproduction analyses without including hadronic form factors [20, 21]. To remind the reader, within 20% symmetry breaking the SU(3) predicts [19]

$$-10.6 \leq g_{K^+\Lambda p} \leq -15.6. \quad (11)$$

TABLE IV

Coupling constants $g_{K^+\Lambda p}$ and $g_{K_1^+\Lambda p}^V$ extracted from the expanded photoproduction amplitude up to n^{th} order in the forward region.

Order	K^+ exchange		K^+ and K_1 exchanges		
	$g_{K^+\Lambda p}$	χ^2/N	$g_{K^+\Lambda p}$	$g_{K_1^+\Lambda p}^V$	χ^2/N
0 th	-5.09	1.10	-5.09	1.49	1.11
2 nd	-5.32	0.88	-9.55	5.93	0.72
4 th	-5.32	0.86	-8.38	5.42	0.72
6 th	-5.32	0.86	-8.89	6.46	0.72
8 th	-5.33	0.86	-9.07	6.79	0.72
10 th	-5.33	0.86	-9.13	6.89	0.72
12 th	-5.33	0.86	-9.15	6.93	0.72
14 th	-5.33	0.86	-9.08	6.79	0.72

The vector-meson coupling $g_{K_1^+\Lambda p}^V$ can also be estimated by utilizing the SU(3) symmetry. However, since the extracted coupling from fitting process is the product $g_{K_1^+K^+\gamma} g_{K_1^+\Lambda p}^V$, there are further uncertainties coming from the determination of the electromagnetic coupling $g_{K_1^+K^+\gamma}$. Thus, we do not pursue to compare our present result with the SU(3) prediction in this case.

By adding the $K_1(1270)$ exchange to the existing K^+ one, the considered coupling constants become the $g_{K^+\Lambda p}$ and $g_{K_1^+\Lambda p}^V$. The extracted values along with the corresponding χ^2 are given in the last three columns of Table IV. It is apparent from this table that the K_1 exchange is very important in the forward angle kaon photoproduction, since by adding the K_1 exchange the χ^2 decreases and the $g_{K^+\Lambda p}$ increases approaching the SU(3) value. To our knowledge, previous calculation has shown that the K_1 exchange is very important to bring the extracted $g_{K^+\Lambda p}$ closer to the SU(3) prediction [22]. Therefore, our present finding corroborates this result.

As stated before, the sign of coupling constants cannot be determined from the numerical calculation. Different from the K_1 exchange, the K^* intermediate state has much smaller contribution in our calculation. The

corresponding couplings, $g_{K^*AN}^V$ and $g_{K^*AN}^T$, should have very large values in order to produce a small effect in the calculated cross section. Thus, we do not show the corresponding values and discuss them here.

Compared to the result obtained from the single t -channel intermediate state, adding the K_1 exchange seems to slow down the convergence rate as can be seen by comparing the second and fourth columns of Table IV. In the single intermediate state, the convergence is already achieved by calculating the amplitude up to the second order. On the contrary, the result obtained from using both K^+ and K_1^+ mesons seems to be not convergent even at the 14th order calculation.

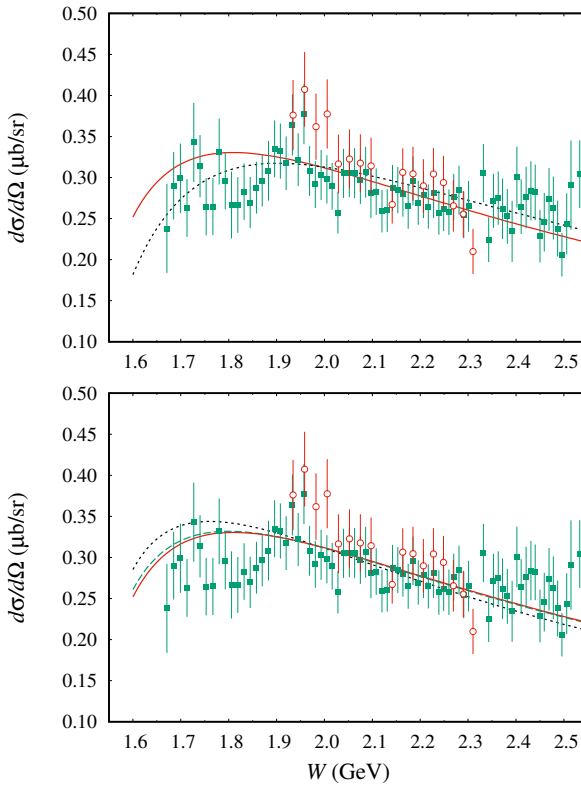


Fig. 4. (Top panel) Differential cross section at the forward direction obtained from the K^+ intermediate state in t -channel (solid line) and from the combination of K^+ and K_1 intermediate states (dotted line). (Bottom panel) Differential cross section at the forward direction obtained from the 0th order (dotted line), 2nd order (dashed line), and 14th order (solid line) expansion. Experimental data are taken from the CLAS Collaboration (solid squares) [16] and LEPS Collaboration (open circles) [23].

The sensitivity of the K_1 exchange is depicted in the top panel of Fig. 4. It is apparent from this panel that the contribution of this state is significant near the threshold region, where its effect is shifting the calculated cross section closer to experimental data. The convergence of the squared amplitude expansion is displayed in the bottom panel of Fig. 4. Obviously, after the second order expansion, the expansion is practically convergent. This is also supported by the fact that the error bars of the present data cannot resolve the differences produced by different order calculations (see the bottom panel of Fig. 4).

To conclude this section, we might safely say that as in the case of the determination of pion electromagnetic form factor from the t -channel pion electroproduction [10], the extraction of the leading kaon coupling constant $g_{K+\Lambda p}$ can be approximated by only using the t -channel intermediate states K and K_1 .

6. Kaon photoproduction at backward angles

In general, the differential cross section obtained from the u -channel contribution is relatively smaller than that obtained from the K^+ exchange in the t -channel. In the backward direction, however, the magnitude of Mandelstam variable $|u|$ is very small and, as a consequence, the corresponding contribution becomes significant and can be expected to dominate all contributions [24]. Note that different from the t -channel term, the u -channel amplitude is individually gauge-invariant, since the exchanged particle Λ is neutral and, therefore, the u -channel amplitude contributes only the magnetic moment term.

Since we have two exchange particles in the u -channel, *i.e.*, Λ and Σ^0 , the unknown parameters in this case are $g_{K+\Lambda p}$ and $g_{K+\Sigma^0 p}$ couplings. These coupling constants were extracted from fitting the kaon photoproduction data with $152^\circ < \theta < 161^\circ$. The result is shown in Fig. 5, where we compare the calculated cross section obtained from the expanded squared amplitude with 0th up to 14th orders with the CLAS 2010 and LEPS 2007 data. From Fig. 5, we can see that the cross sections obtained from expansions with different orders show a large variance only at low energies, where unfortunately no data are available in this kinematics. Therefore, the experimental measurement to this end is strongly required in order to check whether or not the high order expansions are decisive in the backward direction.

The extracted coupling constants along with the corresponding χ^2/N obtained from expansions with different orders are listed in Table V. In contrast to the case of forward angles, in the backward direction both the χ^2/N and the extracted coupling constants are very large. The latter are even much larger than the prediction of SU(3). This result indicates that photoproduction of kaon at the backward angles cannot be explained by merely using the

u -channel. We observe that the coupling constants can be greatly decreased if we add the s -channel contribution. Previous analyses have shown that including hyperon resonances could also alleviate this problem [25, 26].

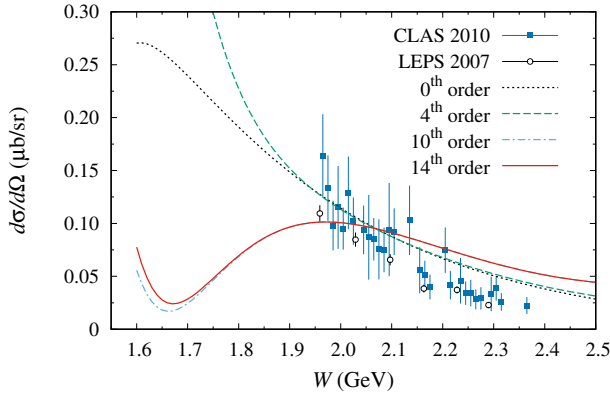


Fig. 5. Differential cross section in the backward direction obtained from different orders of expansion compared with experimental data. Experimental data are taken from the CLAS (open circles [27]) and LEPS (solid squares [12]) collaborations.

TABLE V

The leading coupling constants in $K^+ \Lambda$ photoproduction, $g_{K^+ \Lambda p}$ and $g_{K^+ \Sigma^0 p}$, extracted from the backward angle data for different orders of expansion.

Order	$g_{K^+ \Lambda p}$	$g_{K^+ \Sigma^0 p}$	χ^2/N
0 th	-172.9 ± 62.5	-89.7 ± 34.6	26.3
2 nd	-1.58 ± 1340.3	4.80 ± 697.1	56.6
4 th	-457.7 ± 121.9	-236.8 ± 66.3	27.1
6 th	-694.0 ± 2160.5	-360.1 ± 1152.2	36.8
8 th	-693.3 ± 825.9	-360.2 ± 442.9	33.2
10 th	-695.6 ± 929.4	-361.3 ± 498.0	33.7
12 th	-695.5 ± 926.9	-361.3 ± 496.6	33.7
14 th	-695.5 ± 924.4	-361.3 ± 496.3	33.7

7. Summary and conclusions

We have investigated the convergence of the expansion of squared PV amplitude for kaon photoproduction at threshold. We found that the expanded PV amplitude starts to converge at the 9th order. Should we use solely the zeroth and first order expansions, then the main coupling constant $g_{K \Lambda p}$ must be much smaller than the SU(3) prediction, if the calculated

cross section is fitted to experimental data close to threshold. Therefore, our present investigation concludes that LET using the expansion of lowest order m_K/m would be difficult to derive. We have also extracted the leading coupling constants in kaon photoproduction by expanding the squared PV amplitude at forward and backward directions by solely utilizing the t - and u -channel amplitudes, respectively. It is found that, unless the K_1 vector meson was included, the extracted coupling constants in the forward direction are smaller than the SU(3) prediction. Adding the K_1 significantly improves the agreement of our calculation with the SU(3) prediction. In the backward direction, we found a different result, the extracted coupling constants are much larger than the SU(3) value.

This work has been supported by the PITTA A Grant, Universitas Indonesia, under contract No. NKB-0449/UN2.R3.1/HKP.05.00/2019.

Appendix A

Expansion of the transition amplitude

As described in Sec. 3, we expand the square of the amplitude according to $|\mathcal{M}|^2 = \sum_{n=0}^{20} |\mathcal{M}|_{(n)}^2$, where $|\mathcal{M}|_{(n)}^2 \propto x^n$. To simplify the formulas, we define the following quantities:

$$m = (m_p + m_\Lambda)/2, \quad (\text{A.1})$$

$$x = m_K/m, \quad (\text{A.2})$$

$$y = (m - m_\Sigma)/m \quad (\text{A.3})$$

$$\kappa = \kappa_p + \kappa_\Lambda, \quad (\text{A.4})$$

$$g_\Lambda = eg_{K^+\Lambda p}, \quad (\text{A.5})$$

$$g_\Sigma = eg_{K^+\Sigma^0 p}, \quad (\text{A.6})$$

$$G_\Lambda = \kappa g_\Lambda, \quad (\text{A.7})$$

$$G_\Sigma = \kappa_T g_\Sigma, \quad (\text{A.8})$$

$$G_{K^*} = (G_{K^*}^T + G_{K^*}^V) / Mm_{K^*}^2, \quad (\text{A.9})$$

$$G_{K_1} = G_{K_1}^V / Mm_{K_1}^2. \quad (\text{A.10})$$

The n^{th} order of the expanded amplitude is given by

$$|\mathcal{M}|_{(0)}^2 = 4g_\Lambda^2 + 4g_\Lambda G_\Sigma y^2, \quad (\text{A.11})$$

$$|\mathcal{M}|_{(1)}^2 = -(4g_\Lambda^2 + 4g_\Lambda G_\Sigma y - 2g_\Lambda G_\Sigma y^2) x, \quad (\text{A.12})$$

$$|\mathcal{M}|_{(2)}^2 = [2g_\Lambda(2g_\Lambda + G_\Lambda + G_\Sigma) + G_\Sigma y(g_\Lambda - g_{\Lambda y} + G_{\Lambda y} + 2G_\Sigma y) + 8G_{K_1} m^3 (2g_\Lambda + g_\Sigma y^2)] x^2, \quad (\text{A.13})$$

$$|\mathcal{M}|_{(3)}^2 = \left[\frac{1}{2} (8g_\Lambda^2 + 4g_\Lambda G_\Lambda + 4g_\Lambda G_\Sigma + g_\Lambda G_\Sigma y + 2G_\Lambda G_\Sigma y + 2G_\Sigma^2 y - 2g_\Lambda G_\Sigma y^2 - g_\Lambda G_\Sigma y^2 - 2G_\Sigma^2 y^2) - G_{K^*} m^3 (2g_\Lambda + G_\Sigma y^2) + 4G_{K_1} m^3 (4g_\Lambda + 2G_\Sigma y - G_\Sigma y^2) \right] x^3, \quad (\text{A.14})$$

$$|\mathcal{M}|_{(4)}^2 = - \left[-\frac{1}{16} (4g_\Lambda^2(4+\kappa)^2 + G_\Sigma (4+4y-7y^2) + 2G_\Sigma (16g_\Lambda + 2g_{\Lambda y} - 7g_{\Lambda y}^2 + G_\Lambda (4+2y-2y^2))) + 4G_{K^*} m^3 (3g_\Lambda + G_\Sigma y) - 2G_{K_1} m^3 (10g_\Lambda + 2G_\Lambda + 2G_\Sigma + G_\Sigma y) - 16G_{K_1}^2 m^6 + \frac{8G_{K_1} m^5 (2g_\Lambda + G_\Sigma y^2)}{m_{K_1}^2} \right] x^4, \quad (\text{A.15})$$

$$|\mathcal{M}|_{(5)}^2 = - \left[\frac{1}{8} (2g_\Lambda^2(4+\kappa)^2 + G_\Sigma^2 (2+y+53y^2) + G_\Sigma (16g_\Lambda + g_{\Lambda y} + 2g_{\Lambda y}^2 + G_\Lambda (4+y+26y^2)) + 16G_{K_1}^2 m^6 - G_{K^*} m^3 (2g_\Lambda(8+\kappa) + G_\Sigma (2+3y)) + G_{K_1} m^3 (4g_\Lambda(6+\kappa) + G_\Sigma (4+3y-y^2)) - 16G_{K_1} G_{K^*} m^6 - \frac{4G_{K_1} m^5 (8g_\Lambda + 2G_\Sigma y + G_\Sigma y^2)}{m_{K_1}^2} + \frac{4G_{K^*} m^5 (2g_\Lambda + G_\Sigma y^2)}{m_{K^*}^2} \right] x^5, \quad (\text{A.16})$$

$$|\mathcal{M}|_{(6)}^2 = - \left[-\frac{1}{64} (16g_\Lambda^2(4+\kappa)^2 + G_\Sigma^2 (16+4y-63y^2) + 2G_\Sigma (64g_\Lambda + 2g_{\Lambda y} - g_{\Lambda y}^2 + G_\Lambda (16+2y-15y^2))) - \frac{1}{16} G_\Sigma (-10g_\Lambda + 4G_\Lambda + 11G_\Sigma) y^2 - 16G_{K^*}^2 m^6 - 24G_{K_1}^2 m^6 + 24G_{K^*} G_{K_1} m^6 - 8G_\Sigma G_{K_1} m^3 y^2 - \frac{8G_{K_1} m^7 (2g_\Lambda - 4G_{K_1} m + G_\Sigma y^2)}{m_{K_1}^4} - \frac{4G_{K^*} m^5 (5g_\Lambda + G_\Sigma y + G_\Sigma y^2)}{m_{K^*}^2} - \frac{1}{4} (G_{K_1} m^3 (4g_\Lambda(28+5\kappa) + G_\Sigma (20+12y-37y^2))) + \frac{1}{2} (G_{K^*} m^3 (g_\Lambda(40+6\kappa) + G_\Sigma (6+6y - y^2))) + \frac{2G_{K_1} m^5 (2g_\Lambda(13+\kappa) + G_\Sigma (2+5y+2y^2))}{m_{K_1}^2} \right] x^6, \quad (\text{A.17})$$

$$\begin{aligned}
|\mathcal{M}|_{(7)}^2 = & - \left[\frac{1}{64} (16g_\Lambda^2(4+\kappa)^2 + G_\Sigma^2(16+2y-15y^2) + 2G_\Sigma(64g_\Lambda + g_{\Lambda y} \right. \\
& - 19g_{\Lambda y}^2 + G_\Lambda(16+y-6y^2)) - \frac{4G_{K^*}m^7(2g_\Lambda + G_\Sigma y^2)}{m_{K^*}^4} \\
& - \frac{64G_{K_1}^2m^8}{m_{K_1}^2} + \frac{4G_{K_1}m^7(12eg_\Lambda + 2G_\Sigma y + 3G_\Sigma y^2)}{m_{K_1}^4} \\
& + 16G_{K_1}^2m^6 + \frac{G_{K_1}m^5(-4g_\Lambda(3+2\kappa) + G_\Sigma(8-11y+7y^2))}{m_{K_1}^2} \\
& + \frac{1}{2}(G_{K_1}m^3(4G_\Lambda + G_\Sigma(4-4y+3y^2))) - 36G_{K_1}G_{K^*}m^6 \\
& + 8G_{K^*}^2m^6 + \frac{G_{K^*}m^5(2g_\Lambda(18+\kappa) + G_\Sigma(2+7y+4y^2))}{m_{K^*}^2} \\
& - \frac{1}{8}(G_{K^*}m^3(32g_\Lambda(6+\kappa) + G_\Sigma(32+24y-7y^2))) + 16G_{K_1}^2m^6 \\
& \times G_{K_1}m^3(4g_\Lambda(8+\kappa) + G_\Sigma(4+5y-3y^2))m_{K_1}^2 + \frac{16G_{K^*}G_{K_1}m^8}{m_{K_1}^2} \\
& \left. + \frac{16G_{K^*}G_{K_1}m^8}{m_{K^*}^2} - \frac{4G_{K_1}m^5(16g_\Lambda + 6G_\Sigma y - G_\Sigma y^2)}{m_{K_1}^2} \right] x^7, \tag{A.18}
\end{aligned}$$

$$\begin{aligned}
|\mathcal{M}|_{(8)}^2 = & - \left[-\frac{1}{256} (64g_\Lambda^2(4+\kappa)^2 + G_\Sigma^2(64+4y-49y^2) + 2G_\Sigma(256g_\Lambda \right. \\
& + 2g_{\Lambda y} - 71g_{\Lambda y}^2 + G_\Lambda(64+2y-21y^2)) + 50G_{K_1}G_{K^*}m^6 \\
& + \frac{112G_{K_1}^2m^8}{m_{K_1}^2} - \frac{2G_{K_1}m^7(2g_\Lambda(25+\kappa) + G_\Sigma(2+9y+8y^2))}{m_{K_1}^4} \\
& - \frac{48G_{K_1}^2m^{10}}{m_{K_1}^4} + \frac{8G_{K_1}m^9(2g_\Lambda + G_\Sigma y^2)}{m_{K_1}^8} - 40G_{K_1}G_{K^*}m^8 \\
& + \frac{8G_{K^*}^2m^8}{m_{K^*}^2} + \frac{4G_{K^*}m^7(7g_\Lambda + G_\Sigma y(1+2y))}{m_{K^*}^4} - \frac{40G_{K_1}G_{K^*}m^8}{m_{K^*}^2} \\
& - 13G_{K^*}^2m^6 - \frac{G_{K^*}m^5(+2g_\Lambda(56+5\kappa) + G_\Sigma(10+20y+7y^2))}{2m_{K^*}^2} \\
& + \frac{1}{16}G_{K^*}m^3(16g_\Lambda(28+5\kappa) + G_\Sigma(80+48y-19y^2)) \\
& \left. - 164G_{K_1}^2m^6 + \frac{G_{K_1}m^5(52g_\Lambda(8+\kappa) + G_\Sigma(52+64y+7y^2))}{4m_{K_1}^2} \right]
\end{aligned}$$

$$-\frac{1}{4}G_{K_1}m^3(4g_\Lambda(36+7\kappa)+G_\Sigma(28+12y-7y^2))\Big]x^8, \quad (\text{A.19})$$

$$\begin{aligned} |\mathcal{M}|_{(9)}^2 = & -\left[\frac{1}{128}2(32g_\Lambda^2(4+\kappa)^2+G_\Sigma^2(32+y-21y^2)+G_\Sigma(256g_\Lambda\right. \\ & +g_{\Lambda y}-68g_{\Lambda y}^2+G_\Lambda(64+y-19y^2)) \\ & +\frac{144G_{K_1}^2m^{10}}{m_{K_1}^4}-\frac{4G_{K_1}m^9(16g_\Lambda+2G_\Sigma G_{K_1}m^9y+5G_\Sigma y^2)}{m_{K_1}^6} \\ & -\frac{48G_{K_1}^2m^8}{m_{K_1}^2}+\frac{G_{K_1}m^7(4g_\Lambda(16+3\kappa)+G_\Sigma(12+7y-y^2))}{m_{K_1}^4} \\ & +3G_{K_1}^2m^6+\frac{3G_{K_1}m^5(-4g_\Lambda(4+\kappa)+G_\Sigma(-4+y^2))}{4m_{K_1}^2} \\ & +\frac{1}{32}g_\Lambda G_{K_1}(-1280+8007\kappa)m^3y^2+\frac{4G_{K^*}m^9(2g_\Lambda+G_\Sigma y^2)}{m_{K^*}^6} \\ & -\frac{16G_{K^*}G_{K_1}m^{10}}{m_{K^*}^4}+\frac{76G_{K_1}G_{K^*}m^8}{m_{K^*}^2}-\frac{16G_{K_1}G_{K^*}m^{10}}{m_{K_1}^4} \\ & +152G_{K^*}^2m^6+\frac{G_{K^*}m^5(8g_\Lambda(80+9\kappa)+G_\Sigma(72+104y+21y^2))}{8m_{K^*}^2} \\ & -\frac{24G_{K^*}^2m^8}{m_{K^*}^2}-\frac{G_{K^*}m^7(2g_\Lambda(32+\kappa)+G_\Sigma(2+11y+12y^2))}{m_{K^*}^4} \\ & \times\frac{1}{32}G_{K^*}m^3(64g_\Lambda(16+3\kappa)+G_\Sigma(192+96y-47y^2)) \\ & +48G_{K_1}^2m^6+\frac{G_{K_1}m^5(-4g_\Lambda(31+4\kappa)-G_\Sigma(16+19y+y^2))}{m_{K_1}^2} \\ & +G_{K_1}G_\Sigma m^3(8+3y-2y^2)-\frac{16G_{K_1}G_{K^*}m^{10}}{m_{K_1}^2m_{K^*}^2} \\ & +\frac{1}{32}G_{K_1}m^3(1280g_\Lambda(1+y^2)+G_\Lambda(256-8007y^2)) \\ & -\frac{128G_{K_1}^2m^8}{m_{K_1}^2}+\frac{4G_{K_1}m^7(28eg_\Lambda+6eG_\Sigma y+5eG_\Sigma y^2)}{m_{K_1}^4} \\ & \left. +\frac{76G_{K_1}G_{K^*}m^8}{m_{K_1}^2}-66G_{K_1}G_{K^*}m^6\right]x^9. \quad (\text{A.20}) \end{aligned}$$

REFERENCES

- [1] T. Mart, *Phys. Rev. C* **82**, 025209 (2010).
- [2] T. Mart, *Phys. Rev. C* **83**, 048203 (2011).
- [3] T. Mart, S. Clymton, A.J. Arifi, *Phys. Rev. D* **92**, 094019 (2015).
- [4] S. Clymton, T. Mart, *Phys. Rev. D* **96**, 054004 (2017).
- [5] T. Mart, S. Sakinah, *Phys. Rev. C* **95**, 045205 (2017).
- [6] A.I. Vainshtein, V.I. Zakharov, *Nucl. Phys. B* **36**, 589 (1972).
- [7] G.W. Gaffney, *Phys. Rev.* **161**, 1599 (1967).
- [8] R. Rockmore, *Phys. Rev.* **177**, 2573 (1969).
- [9] S.G. Brown, G.B. West, *Phys. Rev.* **168**, 1605 (1968).
- [10] T. Mart, *Mod. Phys. Lett. A* **23**, 3317 (2008).
- [11] T. Mart, B. Van Der Ventel, *Phys. Rev. C* **78**, 014004 (2008); T. Mart, *Nucl. Phys. A* **815**, 18 (2009); T. Mart, L. Tiator, D. Drechsel, C. Bennhold, *Nucl. Phys. A* **640**, 235 (1998); **631**, 765 (1998).
- [12] K. Hicks *et al.* [LEPS Collaboration], *Phys. Rev. C* **76**, 042201 (2007).
- [13] S.L. Adler, *Phys. Rev.* **139**, 1638 (1965).
- [14] F.X. Lee, T. Mart, C. Bennhold, L.E. Wright, *Nucl. Phys. A* **695**, 237 (2001).
- [15] K.H. Glander *et al.*, *Eur. Phys. J. A* **19**, 251 (2004).
- [16] R. Bradford *et al.* [CLAS Collaboration], *Phys. Rev. C* **73**, 035202 (2006).
- [17] M. Tanabashi *et al.* [Particle Data Group], *Phys. Rev. D* **98**, 030001 (2018).
- [18] M. Guidal, J.M. Laget, M. Vanderhaegen, *Nucl. Phys. A* **627**, 645 (1997).
- [19] R.A. Adelseck, B. Saghai, *Phys. Rev. C* **42**, 108 (1990).
- [20] T. Mart, C. Bennhold, C.E. Hyde-Wright, *Phys. Rev. C* **51**, 1074 (1995).
- [21] R.A. Adelseck, C. Bennhold, L.E. Wright, *Phys. Rev. C* **32**, 1681 (1985).
- [22] R. A. Adelseck, L.E. Wright, *Phys. Rev. C* **38**, 1965 (1988).
- [23] M. Sumihama *et al.* [LEPS Collaboration], *Phys. Rev. C* **73**, 035214 (2006).
- [24] Y. Morino *et al.*, *Prog. Theor. Exp. Phys.* **2015**, 013D01 (2015).
- [25] T. Mart, N. Nurhadiansyah, *Few-Body Syst.* **54**, 1729 (2013).
- [26] W.D. Suciawo, S. Clymton, T. Mart, *J. Phys.: Conf. Ser.* **856**, 012011 (2017).
- [27] M.E. McCracken *et al.* [CLAS Collaboration], *Phys. Rev. C* **81**, 025201 (2010).